Molecular-dynamics simulation of thermal conductivity of silicon crystals

Sebastian G. Volz
Laboratoire d'Etudes Thermiques, UMR 6608 CNRS, Site du Futuroscope, Boîte Postale 109, 86960 Futuroscope Cedex, France

Gang Chen
Mechanical and Aerospace Engineering Department, University of California, Los Angeles, California 90095
(Received 9 April 1999)

We investigate the thermal conductivity of bulk silicon crystals based on molecular-dynamics (MD) simulations. If it is taken that the system size must be larger than the phonon mean free path, several hundreds of millions of atoms must be computed for crystals with large thermal conductivity values such as Si. We demonstrate in this work that the thermal conductivity of Si crystals can be simulated by MD techniques using several thousands of atoms with periodic boundary conditions. We identify that the key issues generating size artifacts in small molecular-dynamics systems are the frequency cutoff imposed by the simulation domain length and the correlation artifacts caused by the periodic boundary conditions. Our method relies on the spectral Green-Kubo formulation combined with a model-based extrapolation. The obtained thermal conductivity results are in good agreement with the reference data. Both the Green-Kubo formulation and the Boltzmann transport equation lead to the prediction that the thermal conductivities of bulk crystals depend on the frequency of the thermal disturbance. This result has important implications for high-frequency electronic devices.

I. INTRODUCTION

The molecular-dynamics (MD) simulation of the thermal conductivity in crystalline solids remains a difficult task due to the perceived limitation of computational power. If it is taken that the simulation domain must be of the order of one mean free path (MFP), for instance, the computation of the thermal conductivity of bulk crystals requires tracing the trajectory of several hundreds of millions of atoms over 10^6 time steps (up to 1 ns with a femtosecond time step), which is difficult even for supercomputers. Some past MD studies on the thermal conductivity are based on nonequilibrium methods that impose a temperature gradient[1–3] or a heat flux.[4–6] Those nonequilibrium methods suffer from the following three main drawbacks:(i) the temperature gradient needs to be sufficiently large to limit the statistical errors, which makes it difficult to determine the reference temperature, (ii) the simulated system size is smaller than the MFP and the final values are found to be size dependent, and (iii) the boundary conditions affect the phonon distribution, leading to false temperature gradients in the vicinity of the interfaces. The equilibrium approach based on the Green-Kubo formulation has also been followed.[7–10] So far, to the best of our knowledge, previous works provided realistic thermal conductivity values only in amorphous structures and crystals, which have low thermal conductivity values and thus short phonon MFP's.

We show that the MD technique can be applied to the thermal conductivity simulation of single-crystal silicon, which has a large thermal conductivity and relatively long phonon mean free path. We choose an approach based on the Green-Kubo formalism, which allows the application of periodic boundary conditions that effectively overcome the limitation of a small simulation domain compared to the phonon MFP. Albeit, we show that this method still involves size artifacts due to the frequency cutoff and the artificial autocorrelation introduced by periodic boundary conditions. The frequency-dependent Green-Kubo formulation is combined with a model-based extrapolation method to provide the necessary corrections. The thermal conductivity of bulk silicon crystal is computed for different system sizes with a maximum atom number reaching 64 000, and at different temperatures also. Our numerical results compared favorably with experimental data on isotopically pure silicon crystals.[11]

In the next section, we present the basic principles of the MD technique and provide details concerning the Stillinger-Weber potential used to compute the thermal properties of a silicon crystal. The following section is devoted to the thermal conductivity derivation according to the Green-Kubo formula. In the last section we provide corrections and compare our results to standard and recent experimental data.

II. THE MOLECULAR-DYNAMICS TECHNIQUE

The classical molecular-dynamics (MD) technique gives a deterministic nonquantum description of an *N*-atom system, considering each atom as a material point of position $\mathbf{r}_i$, velocity $\mathbf{v}_i$, and of constant mass *M*. For atomic systems, Newton's second law describes the particle motion:

$$M\frac{d^2\mathbf{r}_i}{dt^2}=\sum_{j=1,\ j\neq i}^{N}\mathbf{F}_{ij}, \tag{1}$$

where $\mathbf{F}_{ij}$ is the force exerted by atom *j* on atom *i*. The force term is derived from the interatomic potential that must satisfy both nanoscopic and macroscopic requirements. The potential commonly has a two-body-dependent expression including a short-distance repulsive term (according to the Pauli exclusion principle) and a long-distance attractive

term. In silicon, a well-established expression of the nondimensional interatomic potential u_2 takes the following form:[12]

$$u_2(r_{ij}) = A\left[B\left(\frac{r_{ij}}{\sigma}\right) - 1\right]\exp\left[\left(\frac{r_{ij} - r_{\text{cut}}}{\sigma}\right)^{-1}\right], \tag{2}$$

where the constant r_{cut} is the potential cutoff distance above which no interaction occurs, A, B, and q are parameters, and r is the nondimensional interatomic distance. Since the silicon crystal structure is diamondlike, a three-body potential h is introduced to stabilize the correct angular configuration:

$$h_{ijk} = \eta \exp\left[\gamma\left(\frac{r_{ij} - r_{\text{cut}}}{\sigma}\right)^{-1} + \gamma\left(\frac{r_{ik} - r_{\text{cut}}}{\sigma}\right)^{-1}\right] \times (\cos\theta_{jik} + \tfrac{1}{3})^2, \tag{3}$$

where θ_{ijk} is the angle between $\mathbf{r}_{ij}$ and $\mathbf{r}_{ik}$. The parameters A, B, η, γ, and r_{cut} are set by fitting the simulation results of the total energy and the lattice structure to the experimental data. The energy and the distance units are deduced from the observed atomic energy and lattice spacing at 0 K in silicon: $\epsilon = 3.4723 \times 10^{-19}$ J, $\sigma = 0.209\,51$ nm. The parametric form of Eqs. (2) and (3) was proposed without any consideration of the thermal behavior of silicon crystals. However, later tests based on those equations have proven that both the melting temperature and the thermal expansion fit the experimental data with a good accuracy.[13] In addition to the Stillinger-Weber potential, several other potentials, such as the Tersoff potential and those based on the modified-embedded-atom method, have been used in the past to simulate the thermal properties such as the thermal expansion coefficient of Si. Among them, the Stillinger-Weber parametric form gives better agreement with experimental results on the thermal expansion coefficient, which is the main reason why this potential was selected in the present study.

Given initial conditions, Eq. (1) can be solved to provide the position and the velocity of each particle as a function of time, which will be used to compute the system temperature, heat flux, and thermal conductivity. Temperature can be readily calculated from the velocity of each individual atom in the simulation domain since the Boltzmann distribution function allows the straightforward derivation of the mean kinetic energy $\langle E_c \rangle$ in the following way:

$$\langle E_c \rangle = \tfrac{1}{2} M \sum_{i=1}^{N} v_1^2 = \tfrac{3}{2} N k_B T_{\text{MD}}, \tag{4}$$

where k_B is the Boltzmann constant and N is the number of particles in the system. However, the validity of relation (4) depends on three conditions: (1) no temperature constraints are applied; when a temperature gradient is applied, the Boltzmann distribution is perturbed and Eq. (4) becomes an approximation; (2) the total particle momentum of the system vanishes since a nonvanishing total momentum means bulk motion of the particle system, and (3) the heat capacity is not temperature dependent, which is valid for temperatures greater than the Debye temperature. If one compares the simulated MD temperatures in the range 200–500 K to the experimental Debye temperature value $\theta_D = 645$ K of Si, a quantum correction to both the MD temperature and the thermal conductivity must be carried out. Here, we assume that the system energy is twice the kinetic energy according to the equipartition theorem and write the equality.[14]

$$3 N k_B T_{\text{MD}} = \int_0^{\nu_D} D(\nu) n(\nu, T) \hbar \nu \, d\nu, \tag{5}$$

where the right-hand side represents the total phonon energy in the system, D being the density of states. η is the phonon frequency and n defines the phonon occupation number. This term does not include the zero-point energy since the energy of the classical MD system may take the zero value. From Eq. (5), we deduce the real system temperature T appearing in the function n. Since the temperature gradient in the Fourier law must also be corrected, the thermal conductivity λ_{MD} should be rescaled by the $\partial T_{\text{MD}}/\partial T$ factor obtained from Eq. (5). When the system temperature is close the to Debye temperature, the correction is not sensitive to the exact values of this parameter. Taking θ_D values of 645 and 722 K, for instance, the discrepancies in the temperature values T are 6% and 4% in the correction coefficient $\partial T_{\text{MD}}/\partial T$. In the framework of the quantum correction procedure used here, the change in the Debye temperature will therefore not have a significant influence on the results.

The heat-flux expression is derived from the energy-balance equation:

$$\frac{1}{V}\frac{\partial E(\mathbf{r}, t)}{\partial t} + \nabla \cdot \mathbf{q}(\mathbf{r}, t) = 0, \tag{6}$$

where $E(\mathbf{r}, t)$ is the instantaneous local energy and $\mathbf{q}(\mathbf{r}, t)$ the instantaneous local heat flux. The integration of Eq. (6) combined with the definition of the total instantaneous heat flux in the statistical ensemble of constant energy leads to the following expression:[15,16]

$$\mathbf{q}(t) V = \frac{d}{dt} \sum_i \mathbf{r}_i E_i \tag{7}$$

where E_i is the particle energy and V the system volume. When expressing E_i in terms of the atomic kinetic and potential energies (ϕ_{ij}), $E_i = \frac{1}{2}(M v_i^2 + \phi_{ij})$, Eq. (7) becomes

$$\mathbf{q}(t) = \frac{1}{V}\left[\sum_{i=1}^{N}\left(\mathbf{v}_i E_i + \tfrac{1}{2}\sum_{j=1,\ j\neq i}^{N} \mathbf{r}_{ij} \cdot (\mathbf{F}_{ij} \cdot \mathbf{v}_i)\right)\right] \tag{8}$$

The first term on the right-hand side is related to local particle shifts typically occurring in fluids, while the second term describes the thermal energy dissipated between groups of atoms, which is dominant in solids. As shown previously, the force potential of silicon includes a three-body contribution that must be taken into account in the path from Eq. (7) to Eq. (8). Thus, we finally obtain the heat-flux expression as follows:

$$\mathbf{q}(t) = \frac{1}{V}\left[\sum_{i=1}^{N}\sum_{j=1,\ j\neq i}^{N}\left(\tfrac{1}{2}\mathbf{r}_{ij} \cdot (\mathbf{F}_{ij} \cdot \mathbf{v}_i) + \tfrac{1}{6}\sum_{k=1,\ k\neq i,j}^{N} (\mathbf{r}_{ij} + \mathbf{r}_{ik}) \cdot (\mathbf{F}_{ijk} \cdot \mathbf{V}_i)\right)\right] \tag{9}$$

where the three-body force term is $\mathbf{F}_{ijk} = -\epsilon \nabla_{r_i}[h(r_{ij}, r_{ik}, \theta_{jik}) + h(r_{ji}, r_{jk}, \theta_{ijk}) + h(r_{ki}, r_{kj}, \theta_{ikj})]$.

III. SPECTRAL THERMAL CONDUCTIVITY

Due to the atomic motion, both local and total quantities $\mathbf{q}_0(\mathbf{r},t)$, $E_0(\mathbf{r},t)$, $\mathbf{q}_0(t)$, and $T_0(t)$ fluctuate around their equilibrium mean values and follow the local energy balance equation (6).[17] We perform the thermal conductivity simulations based on the equilibrium fluctuations of the heat flux $\mathbf{q}_0(t)$.[18,19] In this perspective, a microscopic temperature nonhomogeneity $\delta T(\mathbf{r},t)$ is created in the system and superimposed to the equilibrium fluctuations of the local temperature $T_0(\mathbf{r},t)$. This temperature perturbation creates a deviation of the average energy of the system:

$$\delta E(t) = \frac{k_B T_0}{V} \int_V \frac{E_0(\mathbf{r},t)}{k_B[T_0 + \delta T(\mathbf{r},t)]} dV - E_0 = -\frac{1}{T_0 V} \int_V \delta T(\mathbf{r},t) E_0(\mathbf{r},t) dV, \quad (10)$$

where T_0 is the equilibrium temperature and $E_0(\mathbf{r},t)$ the local equilibrium energy. This energy disturbance causes an instantaneous heat flux in the simulation domain. The resultant heat flux can be expressed in terms of the perturbation of the distribution function:

$$\mathbf{q}(t) = \frac{1}{V} \int_V \mathbf{q}_0(\mathbf{r},t) \rho(t) dV = \frac{1}{V} \int_V \mathbf{q}_0(\mathbf{r},t)\, \delta\rho(t) dV + \mathbf{q}_0(t) \quad (11)$$

where $\delta\rho(t) = -\rho_0(\delta E(t)/k_B T_0)$ is the first-order approximation of the Boltzmann distribution function $\rho(t) = \exp\{-[E_0 + \delta E(t)]/k_B T_0\}$. The last step consists of the reformulation of Eq. (11), replacing $\delta\rho(t)$ by its expression and combining Eqs. (10) and (11). The resulting expression of the spectral thermal conductivity is a consequence of the fluctuation-dissipation theorem:[8,9]

$$\lambda(\mathbf{k},\omega) = \frac{V}{3k_B T_0^2} \int_0^\infty \langle \mathbf{q}_0(\mathbf{k},0) \cdot \mathbf{q}_0(\mathbf{k},t) \rangle e^{i\omega t} dt, \quad (12)$$

where ω and $\mathbf{k}$ are the frequency and wave vector of the external thermal perturbation exerted on the system, $\delta T(\mathbf{r},t) = \delta T e^{i(\omega t - \mathbf{k}\cdot\mathbf{r})}$,

$$\langle \mathbf{q}_0(\mathbf{k},0) \mathbf{q}_0(\mathbf{k},t) \rangle = \frac{1}{V} \int_V \mathbf{q}_0(\mathbf{r},0),$$

$\mathbf{q}_0(\mathbf{r},t) e^{-i\mathbf{k}\cdot\mathbf{r}} \rho_0 dV$ is the heat-flux autocorrelation function, and T_0 is the equilibrium temperature. This last equation is called the spectral Green-Kubo formula for thermal conductivity.[20] It reduces straightforwardly to the static thermal conductivity λ by setting $\mathbf{k}$ and ω to zero. In the past, thermal conductivity simulations were mostly based on the static formula.

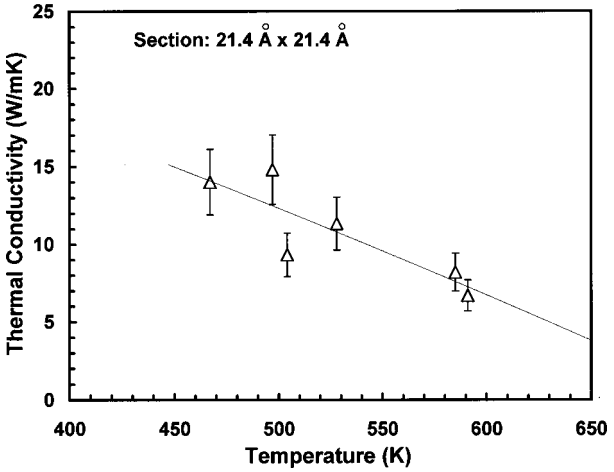

FIG. 1. Bulk thermal conductivity results computed from MD simulations for different temperatures and for a system with a cross section of 4.58 nm^2. The method is based on the static Green-Kubo formulation.

IV. RESULTS AND DISCUSSION

To perform MD computations of the bulk thermal conductivity, we construct the simulation domain from unit cells. Each unit cell is face-centered cubic with two atoms as the basis. We compute systems with cross sections ranging from 3×3 to 10×10 cells and 12 cells in the longitudinal direction. A maximum of $20\times20\times20$ cells was also probed to examine the size artifacts. These simulations correspond to atom numbers ranging from 864 to 64 000 since a diamondlike cell includes eight atoms. We assumed periodic boundary conditions in the three directions and imposed the silicon density by setting the lattice constant a to 0.543 nm. The periodic boundary conditions allow the energy to flow through the boundaries while ensuring the conservation of momentum and energy, i.e., the energy flowing out of one surface will reenter from other surfaces. Therefore, we postulate that such periodic boundary conditions provide the correct representation of the bulk crystal phonon scattering in a simulation domain much smaller than the mean free path. The time unit is defined from the derivation of the nondimensional form of the motion equation: in silicon, $t_u = 0.0766$ ps. For the time step, we chose $dt = 0.01 t_u$, which guarantees a negligible total-energy drift due to the numerical integration scheme. We probed the temperature dependency of the silicon crystal thermal conductivity. It was considered reasonable to extend the time of the simulation to several phonon mean relaxation times $\approx$76 ps, which corresponds to 100 000 time steps. For a $21.4\times21.4\times64.2$ Å^3 crystal with 1536 atoms, the average computation time is 5 h using a HP9000-C180 workstation.

Figure 1 shows the thermal conductivity values derived from the direct integration of the heat-flux autocorrelation function corresponding to the Green-Kubo formulation [Eq. (12)], setting the frequency ω and the wave vector $\mathbf{k}$ to 0, i.e., the static Green-Kubo formula. The thermal conductivity values are one order of magnitude smaller than the reported bulk data $\lambda = 80$ W/mK at 500 K. Figure 2 demonstrates that a further increase in the computation size will increase the calculated thermal conductivity value. For a simulation do-

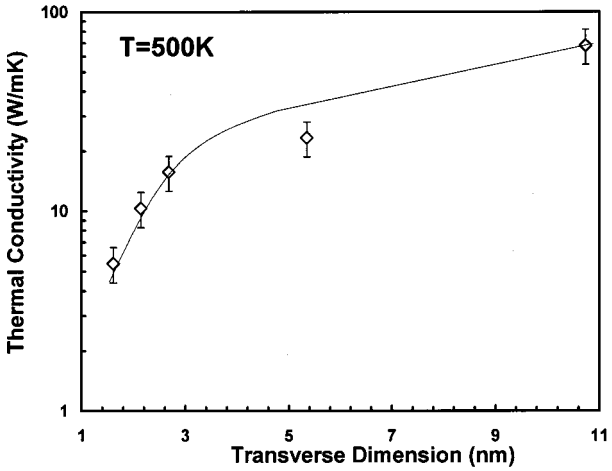

FIG. 2. Thermal conductivity plotted against lateral simulation box dimensions at $T=500$ K. Results remain increasing as the simulation domain increases.

main of $109\times109\times109\text{Å}^3$, the thermal conductivity is about 70 W/mK, while the experimentally reported thermal conductivity of natural Si (with 5–10 % isotopes) at 500 K is about 80–90 W/mK. This justifies the belief that the size effect is responsible for the small simulated thermal conductivity values compared with experimental data. Since the periodic boundary condition should have at least partially compensated the MFP limit, we infer that other effects exist, further limiting the calculated thermal conductivity values. To examine the artifacts induced by the small simulation domain V and the periodic boundary conditions, we express the spectral thermal conductivity $\lambda(\mathbf{k},\omega)$, as a function of the heat-flux fluctuations occurring in the basic cell:

$$\lambda(\mathbf{k},\omega)=\frac{V_{\text{mac}}}{3k_BT_0^2}\int_0^\infty\frac{1}{V}\int_V\mathbf{q}_0(\mathbf{r},t)\cdot\mathbf{q}_0(\mathbf{r},0)\rho_0 \times e^{-i\mathbf{k}\cdot\mathbf{r}}dVJ(\mathbf{k})e^{i\omega t}dt, \tag{13}$$

where V_{mac} is a macroscopic volume including a large number of volumes V and $J(\mathbf{k})$ is a function including the contributions of the image volumes to the $\langle\mathbf{q}_0(\mathbf{k},t)\mathbf{q}_0(\mathbf{k},0)\rangle$ term. Equation (13) leads to the identification of two opposing size artifacts. First, because the space projection for the space Fourier transform is limited to volume V, only phonons with a wavelength shorter than the cell size are permitted to exist in the simulation domain. This wavelength cutoff has the following two consequences. One is that the contribution of low-wavelength phonons to the thermal conductivity is excluded. The other, which is more important, is that the static disturbance values, $k=0$ and $\omega=0$, are not allowed at all in the simulation domain. Second, since the J function limit when k goes to zero is one instead of zero, an artificial autocorrelation that does not exist in real systems is introduced. This size effect will be especially strong for long-wavelength phonons or low wave vectors k.

We correct the above-identified artifacts caused by the periodic boundary conditions from the spectral Green-Kubo formulation for thermal conductivity. Starting from the high-frequency thermal conductivity, we propose to derive the static value according to an extrapolation method.[21] We build the extrapolation procedure by approximating the heat-flux autocorrelation function expression. The time evolution of the autocorrelation function for the phonon occupation number n_ν is documented as[22]

$$\langle n_\nu(0)n_\nu(t)\rangle=\langle n_\nu,(0)^2\rangle e^{-1/\tau_\nu}, \tag{14}$$

where τ_ν is the relaxation time corresponding to the modes with a frequency ν. Using this time evolution, the time dependence of the heat-flux autocorrelation function

$$\langle\mathbf{q}(0)\mathbf{q}(t)\rangle=\langle q(0)^2\rangle e^{-t/\tau} \tag{15}$$

is derived when assuming no cross-correlation between modes and according to the definition of the heat flux in terms of the phonon occupation numbers

$$\mathbf{q}(t)=\sum_i n_{\nu_i}(t)\hbar\nu_i\mathbf{v}_{\nu_i}, \tag{16}$$

where $\mathbf{v}_\nu$ is the group velocity. In Eq. (15), τ is the average phonon relaxation time assumed to be frequency independent. By combining Eqs. (12) and (15), the spectral thermal conductivity is finally expressed as

$$|\lambda(\omega)|=V\langle q(0)^2\rangle/[3k_BT^2\sqrt{\omega^2+\tau^{-2}}]. \tag{17}$$

By fitting the high-frequency values of $|\lambda(\omega)|$ calculated from spectral MD simulations, the heat-flux autocorrelation relaxation time τ is determined and used to estimate the static thermal conductivity $\lambda(0)$. The mean relaxation time approximation implies that slow and fast disturbances are governed by the same average relaxation time, i.e., the long- and short-wavelength phonons behave similarly. However, we argue that a relatively small simulation domain could represent the Brillouin zone reasonably well. To illustrate this point, we compute the dispersion curves of longitudinal phonons using a classical method[23] that provides the dynamical structure factor $S(\mathbf{k},\nu)$ for the wave vector $\mathbf{k}$ from the time-dependent positions of each particle $\mathbf{r}_i(t)$ according to the relation

$$S(\mathbf{k},\nu)=\int_{-\infty}^{+\infty}dt\sum_n e^{i\nu\tau}e^{i\mathbf{k}\cdot\mathbf{r}_i}, \tag{18}$$

Choosing a set of wave vectors in the Brillouin zone, we plotted in Fig. 3 the dispersion curves of the longitudinal acoustic (LA) phonons in the transverse (crosses) and longitudinal (squares) directions of the simulated rectangular domain. This figure reveals that phonon modes of wavelengths greater than the system size are truncated as shown by the three data points of lower wave vectors reporting LA phonons in the transverse direction (crosses). We verify that the corresponding cutoff frequency is smaller than the frequency of the dominant phonon modes. On the other hand, four unit cells in the transverse direction correctly represent three-fourth's of the phonons in the first Brillouin zone. The extrapolation of Eq. (17) seems therefore reasonable but will likely to be valid only in the high-temperature regimes where short-wavelength phonons dominate. The fact that the classical MD technique cannot correctly represent the scattering mechanisms at low temperature also limits the proposed technique to the high-temperature regime. Incidently, we notice that the calculated frequency for the zone boundary is 8% higher than the reference,[24] while the dynamical matrix

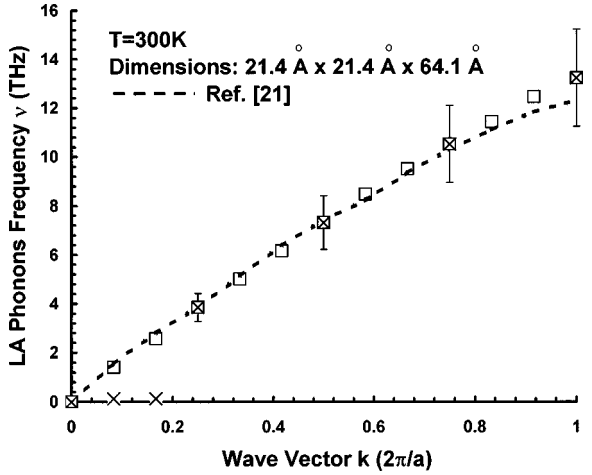

FIG. 3. Dispersion curves of longitudinal acoustic phonons in the transverse (crosses) and longitudinal (squares) directions of a $4\times4\times12$ rectangular simulation domain.

of the Stillinger-Weber potential predicts a frequency value 12.5% smaller than the same reference.[25]

Insofar as the Boltzmann transport equation (BTE) fully describes energy transfers when phonons can be treated as a gas of particles, we will show next that the thermal conductivity expression [Eq. (17)] can also be deduced from the BTE. We start from the basic one-dimensional BTE written under the relaxation time approximation

$$\frac{\partial n_\nu}{\partial t}+v_{x\nu}\frac{\partial n_{0\nu}}{\partial x}=-\frac{n_\nu-n_{0\nu}}{\tau_\nu}, \tag{19}$$

where the 0 index indicates that the equilibrium quantity is considered. Since $n_{0\nu}$ depends on the temperature only, the spatial gradient can be decomposed as the product of the temperature derivative of n_0 and the spatial temperature gradient, which corresponds to the applied thermal disturbance. Choosing an ac perturbation of frequency ω, $T(x,t)=T_0(x)e^{i\omega t}$, the phonon distribution function n will have the form $n(x,t)=H(x,\omega)e^{i\omega t}$. From Eq. (19), $H(x,\omega)$ can be obtained as

$$H(x,\omega)=\frac{n_{0\nu}+v_{x\nu}\tau_\nu(\partial n_{0\nu}/\partial T)(\partial T_0/\partial x)}{1+i\omega\tau_\nu}, \tag{20}$$

which leads to the expression of the complex heat flux:

$$q(x,\omega)=\int_\nu H(x,\omega)\hbar\nu D(\nu)v_{x\nu}d\nu$$

$$=\frac{\partial T_0}{\partial x}\int_\nu\frac{\partial[n_{0\nu}\hbar\nu D(\nu)]}{\partial T}\frac{\tau_\nu v_{x\nu}^2}{1+i\omega\tau_\nu}d\nu. \tag{21}$$

Assuming a frequency-independent relaxation time τ and group velocity, the complex spectral thermal conductivity expression of Eq. (17) is retrieved:

$$\lambda(\omega)=\frac{C_p v_x^2\tau}{1+i\omega\tau}=\frac{\lambda(0)}{1+i\omega\tau}, \tag{22}$$

where $\lambda(0)$ is the static thermal conductivity and C_p is the heat capacity or the temperature derivative of energy.

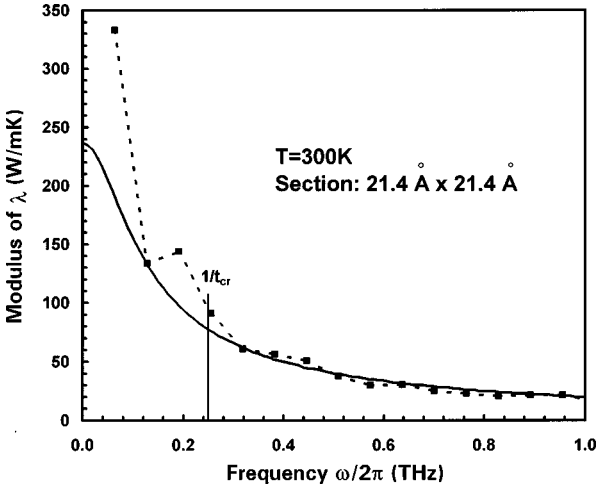

FIG. 4. Modulus of the spectral thermal conductivity of silicon derived from MD simulations (dashed line) and extrapolation to the dc thermal conductivity (solid line). The t_{cr} time approximately corresponds to the minimum frequency allowed in the simulation domain.

Figure 4 shows the frequency dependence of the spectral thermal conductivity obtained from the MD simulations (squares) and its corresponding extrapolation curve (solid line). The simulation results diverge when approaching the frequency $\omega=0$. We understand that this trend is related to the overestimation of the autocorrelation function for low frequencies due to correlation artifacts caused by the periodic boundary conditions. The higher-frequency data are favorably compared to the results of Fig. 1, reinforcing our argument that the static Green-Kubo formulation is not appropriate when the simulation domain is small. To fit the high-frequency regime, the key point is to recognize where the artifacts caused by the periodic boundary conditions appear. The vertical line in the figure marks an estimation of the time t_{cr} required for phonons propagate across the simulation domain ballistically. In the wave picture, t_{cr} is also proportional to the reverse of the minimal frequency allowed in the system. For frequencies higher than this mark, phonons will be scattered and the effects of the artificial correlation will diminish. Figure 5 shows that the corrected thermal conductivity values are not size dependent anymore, which confirms that the results shown in Fig. 1 are truncated because of the low-frequency cutoff.

Figure 6 reports the extrapolation values in configurations comparable to those of Fig. 1. The simulation results suggest that the crystal thermal conductivity decreases with temperature according to a T^{-n} law with the power factor $n=1.5$. Here, n differs from the factors deduced from the standard theory ($n=1$) and the recent measurement on isotopically pure silicon ($n=1.6$).[11] At 300 K, the MD data value is about 70% higher than the thermal conductivity of natural Si but corresponds very well to the experimental results.[11] To complete the discussion, we also plotted the curve extrapolated from this data point and a T^{-1} law. The interval defined by this extrapolation and the results on isotopically pure silicon provides a satisfying framing of our MD values.

V. CONCLUSION

This study provides a simple method to derive the thermal conductivity of bulk crystals with high thermal conductivi-

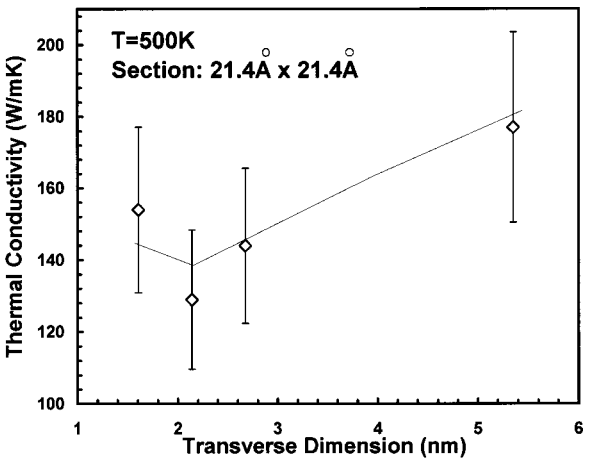

FIG. 5. Corrected thermal conductivity plotted against lateral simulation box dimensions at $T = 500$ K. Results are independent of the crystal size.

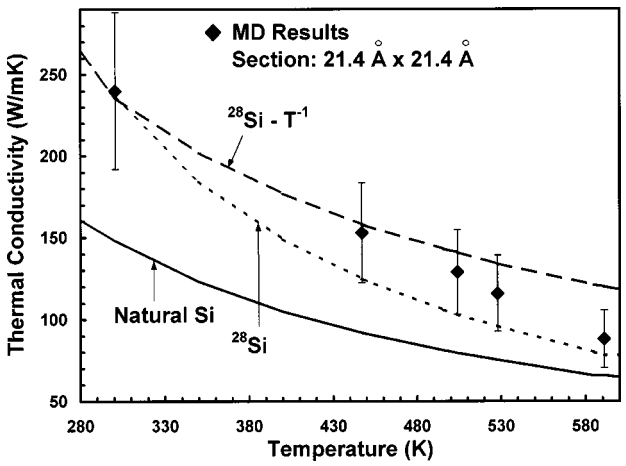

FIG. 6. Bulk thermal conductivity results computed from MD simulations for different temperatures and for a system section of 4.58 nm^2. The MD calculation (squares) is based on the Green-Kubo formulation and the extrapolation technique.

ties from the trajectories of a reduced number of atoms. We found out that the mean-free-path limitation imposed by the system size can be assumed as insignificant when using periodic boundary conditions while the low-frequency cutoff and the artificial correlation involved by the periodic boundary conditions severely affect the noncorrected estimations. Our method relies on the spectral thermal conductivity given by the Green-Kubo formula and an extrapolation technique. The extrapolation procedure is relevant in the high-temperature regime where dominant phonon modes are not cut off and the classical MD technique is approximately valid in taken account of the phonon scattering. The simulation results on the thermal conductivity of Si crystals compare favorably with experimental data on isotopically enriched Si.

ACKNOWLEDGMENTS

This work was partially supported by NSF (G.C.), a DOD/ONR MURI grant on thermoelectricity, and the Laboratoire d'Etudes Thermiques (ENSMA, France). This work was partially performed at UCLA.

[1] A. Tenebaum, G. Ciccotti, and R. Gallico, Phys. Rev. A **25**, 2778 (1982).
[2] S. Kotake and S. Wakuri, JSME Int. J. Ser. B **37**, 103 (1994).
[3] R. D. Mountain and R. A. MacDonald, Phys. Rev. B **28**, 3022 (1983).
[4] T. Ikeshoji and B. Hafskjold, Mol. Phys. **81**, 251 (1994).
[5] F. Muller-Plathe, J. Chem. Phys. **106**, 6082 (1997).
[6] J. Michalski, Phys. Rev. B **45**, 7054 (1992).
[7] R. H. Poetzsch and H. Boettger, Phys. Rev. B **50**, 15 757 (1994).
[8] R. Kubo, J. Phys. Soc. Jpn. **12**, 570 (1957).
[9] R. Kubo and M. Yokota, J. Phys. Soc. Jpn. **12**, 1203 (1957).
[10] R. Zwanzig, Annu. Rev. Phys. Chem. **16**, 67 (1964).
[11] W. S. Capinski, H. Maris, E. Bauser, I. Silier, M. Asen-Palmer, T. Ruf, M. Cardona, and E. Gmelin, Appl. Phys. Lett. **71**, 2109 (1997).
[12] F. H. Stillinger and T. A. Weber, Phys. Rev. B **31**, 5262 (1985).
[13] S. J. Cook and P. Clancy, Phys. Rev. B **47**, 7686 (1993).
[14] A. Maiti, G. D. Mahan, and S. T. Pantelides, Solid State Commun. **102**, 517 (1997).
[15] P. B. Allen and J. L. Feldman, Phys. Rev. B **48**, 12 581 (1993).
[16] R. J. Hardy, Phys. Rev. **132**, 168 (1963).
[17] J. P. Boon and S. Yip, *Molecular Hydrodynamics* (Dover, New York, 1980).
[18] A. J. C. Ladd, B. Moran, and W. G. Hoover, Phys. Rev. B **34**, 5058 (1986).
[19] S. Volz, J. B. Saulnier, M. Lallemand, B. Perrin, P. Depondt, and M. Mareschal, Phys. Rev. B **54**, 340 (1996).
[20] R. Kubo, M. Toda, and N. Hashitsume, *Statistical Physics II* (Springer, Berlin, 1985), p. 194.
[21] Y. Hee Lee, R. Biswas, C. M. Soukoulis, C. Z. Wang, C. T. Chan, and K. M. Ho, Phys. Rev. B **43**, 6573 (1991).
[22] G. P. Srivastava, *The Physics of Phonons* (Hilger, Bristol, 1990).
[23] R. Meyer and P. Entel, Phys. Rev. B **57**, 5140 (1998).
[24] P. Giannozzi, S. Gironcoli, P. Pavone, and S. Baroni, Phys. Rev. B **43**, 7231 (1991).
[25] K. Ding and H. C. Andersen, Phys. Rev. B **34**, 6987 (1986).